Leena P. Bharath,[1,2,3] Ting Ruan,[1,2] Youyou Li,[1,2] Anindita Ravindran,[1,2] Xin Wan,[1,2] Jennifer Kim Nhan,[1,2] Matthew Lewis Walker,[1,2] Lance Deeter,[1,2] Rebekah Goodrich,[1,2] Elizabeth Johnson,[1,2] Derek Munday,[1,2] Robert Mueller,[1,2] David Kunz,[1,2] Deborah Jones,[2] Van Reese,[4] Scott A. Summers,[5] Pon Velayutham Anandh Babu,[1] William L. Holland,[6] Quan-Jiang Zhang,[7] E. Dale Abel,[7] and J. David Symons[1,2,3]

Ceramide-Initiated Protein Phosphatase 2A Activation Contributes to Arterial Dysfunction In Vivo

Diabetes 2015;64:3914–3926 | DOI: 10.2337/db15-0244

Prior studies have implicated accumulation of ceramide in blood vessels as a basis for vascular dysfunction in diet-induced obesity via a mechanism involving type 2 protein phosphatase (PP2A) dephosphorylation of endothelial nitric oxide synthase (eNOS). The current study sought to elucidate the mechanisms linking ceramide accumulation with PP2A activation and determine whether pharmacological inhibition of PP2A in vivo normalizes obesity-associated vascular dysfunction and limits the severity of hypertension. We show in endothelial cells that ceramide associates with the inhibitor 2 of PP2A (I2PP2A) in the cytosol, which disrupts the association of I2PP2A with PP2A leading to its translocation to the plasma membrane. The increased association between PP2A and eNOS at the plasma membrane promotes dissociation of an Akt-Hsp90-eNOS complex that is required for eNOS phosphorylation and activation. A novel small-molecule inhibitor of PP2A attenuated PP2A activation, prevented disruption of the Akt-Hsp90-eNOS complex in the vasculature, preserved arterial function, and maintained normal blood pressure in obese mice. These findings reveal a novel mechanism whereby ceramide initiates PP2A colocalization with eNOS and demonstrate that PP2A activation precipitates vascular dysfunction in diet-induced obesity. Therapeutic strategies targeted to reducing PP2A activation might be beneficial in attenuating vascular complications that exist in the context of type 2 diabetes, obesity, and conditions associated with insulin resistance.

Obesity, type 2 diabetes, and insulin resistance are characterized by endothelial dysfunction (1,2). Progress has been made in elucidating general mechanisms responsible for the mismatch between the synthesis and degradation of nitric oxide (NO) that precipitates endothelial dysfunction (2). A recent focus of our laboratory concerns the contribution to endothelial cell (EC) dysfunction from elevated free fatty acids (FFAs) in general (3) and from the FFA metabolite ceramide in particular (4).

When FFAs are elevated experimentally in control subjects to levels that circulate in patients with metabolic syndrome, endothelium-dependent dysfunction is observed (5–7). Earlier, we reported that FFAs increase approximately threefold when C57Bl6 mice consume standard versus high-fat chow for 12 weeks, in parallel with endothelial dysfunction and hypertension (3). When tissues not suited for lipid storage (e.g., skeletal muscle, liver, arteries) are exposed to elevated FFAs, the toxic bioactive sphingolipid ceramide increases and heightens cardiovascular risk (4,8,9). Prevention of arterial ceramide accumulation

[1]College of Health, The University of Utah, Salt Lake City, UT
[2]Division of Endocrinology, Metabolism and Diabetes, The University of Utah School of Medicine, Salt Lake City, UT
[3]Molecular Medicine Program, The University of Utah School of Medicine, Salt Lake City, UT
[4]The University of Utah Geriatric Research, Education, and Clinical Center, George E. Wahlen VA Medical Center, Salt Lake City, UT
[5]Baker IDI Heart and Diabetes Institute, Melbourne, Australia
[6]Touchstone Diabetes Center, The University of Texas Southwestern Medical Center, Dallas, TX
[7]Fraternal Order of Eagles Diabetes Research Center and Division of Endocrinology and Metabolism, Roy J. and Lucille A. Carver College of Medicine, The University of Iowa, Iowa City, IA

Corresponding author: J. David Symons, j.david.symons@hsc.utah.edu.

Received 22 February 2015 and accepted 17 July 2015.

This article contains Supplementary Data online at http://diabetes.diabetesjournals.org/lookup/suppl/doi:10.2337/db15-0244/-/DC1.

in arteries from fat-fed mice using pharmacological and genetic approaches attenuates endothelial dysfunction and systemic hypertension (4). Molecular mechanisms examined in ECs reveal that palmitate-evoked ceramide biosynthesis induces colocalization of type 2 protein phosphatase (PP2A) with endothelial NO synthase (eNOS) and disrupts an Akt-Hsp90-eNOS complex leading to reduced eNOS phosphorylation and NO generation. Congruent with these findings in ECs, increased ceramide-dependent association of PP2A with eNOS in immunoprecipitates of arterial lysates from fat-fed mice is observed (4).

The current study sought to elucidate the mechanism whereby ceramide accrual initiates colocalization of the Ser/Thr phosphatase PP2A with eNOS. In ECs treated with palmitate, multiple approaches were used to show that de novo synthesized ceramide colocalizes with the inhibitor 2 of PP2A (I2PP2A) in the cytosol. The I2PP2A-mediated cytosolic retention of PP2A is inhibited leading to translocation of PP2A to the plasma membrane where it associates with membrane-localized eNOS. These defects could be ameliorated in palmitate-treated ECs by pharmacological and genetic procedures that limit endogenous ceramide biosynthesis, prevented in palmitate-treated ECs that were transfected with catalytically inactive mutant PP2A, and recapitulated in vehicle-treated ECs after small interfering RNA (siRNA)-mediated suppression of I2PP2A gene expression.

Although we (4) and others (10,11) have shown that PP2A inhibition may preserve eNOS phosphorylation and maintain eNOS enzyme function in high-fat–fed animals, it remains to be determined whether PP2A inhibition can prevent arterial dysfunction in diet-induced obesity and hypertension in vivo. Findings presented herein show that a potent and selective small-molecule inhibitor of PP2A (12–14) limits palmitate-induced increases in PP2A activity, prevents disruption of the vascular Akt-Hsp90-eNOS complex, and thereby preserves NO generation in ECs. Moreover, inhibiting PP2A activity in vivo maintains the Akt-Hsp90-eNOS complex in the vasculature and prevents endothelial dysfunction and hypertension caused by 6 h of lard oil infusion or by 12 weeks of fat feeding. Collectively, these findings elucidate a novel mechanism whereby ceramide initiates PP2A colocalization with eNOS, revealing how PP2A activation can precipitate lipid or obesity-induced vascular dysfunction, and demonstrate that small-molecule inhibition of PP2A can prevent the associated vascular dysfunction.

RESEARCH DESIGN AND METHODS

Cell Studies

Bovine aortic endothelial cells were purchased (Lonza, Inc., Allendale, NJ) and were grown in DMEM supplemented with 10% FBS in a humidified atmosphere (5% CO_2, 95%O_2) at 37°C. At 70–80% confluency, cells were passaged and transferred to culture plates. Palmitate (C16:0) was coupled to fatty acid–free BSA in the ratio of 2 mol palmitate to 1 mol BSA (3,4,15). ECs were treated for 3 h with *1*) 1% BSA (vehicle), *2*) 1% BSA plus 10 μmol/L myriocin, *3*) vehicle plus 500 μmol/L palmitate, *4*) myriocin plus palmitate, *5*) vehicle plus 4 μmol/L LB100 (LB1), or *6*) LB1 plus palmitate. Myriocin inhibits Ser palmitoyl transferase (16), and LB1 inhibits the Ser/Thr phosphatase PP2A (12–14,17). For some experiments, ECs were treated with *1*) 100 nmol/L insulin to stimulate phosphorylated (p-)eNOS^{Ser1177} (3,4); *2*) 10 μmol/L FTY720, a sphingolipid analog; *3*) 3 μmol/L tautomycin to inhibit PP1; or *4*) 100 nm cyclosporine to inhibit PP2B (18,19). After 3 h, the following experiments were completed.

Ceramide Biosynthesis

Immunofluorescence and confocal microscopy were used to assess endogenous ceramide accumulation (10).

PP2A Activity

PP2A activity was evaluated after immunoprecipitation of the catalytic (C) subunit of PP2A (PP2A-C) using a malachite green phosphatase assay kit (Millipore, Billerica, MA) or by measuring phosphorylation of tyrosine (Tyr) 307 to total PP2A (p-PP2A^{Tyr307}:PP2A) by immunoblot.

Mutant Transfection

ECs were transfected with either wild-type hemagglutinin (HA)-tagged PP2A-C (wt) plasmid or HA-tagged catalytic site mutant PP2A-C plasmid (mut) (20) using Lipofectamine 3000 reagent (Life Technologies, Grand Island, NY).

siRNA Generation and Transfection

siRNA for knockdown of I2PP2A was performed using Lipofectamine 2000 and standard procedures (21).

Immunoblotting

ECs and arteries were processed for immunoprecipitation and immunoblotting as we have previously described (3,4,22,23).

EC Fractionation

Cells were lysed, homogenized, and centrifuged at 1,000*g* for 10 min using a modification of a previous method (24). The supernatant was collected and centrifuged at 100,000*g* for 60 min at 4°C. The pellet was washed and prepared for immunoblotting as previously described (3,4,22,23).

NO Production

NO was assessed using ELISA (Abcam, Cambridge, MA) and electron paramagnetic spin resonance (EPR) as we previously described (3,4).

Genotyping

Genotyping of mice haploinsufficient for dihydroceramide desaturase (i.e., des1$^{+/-}$ mice [HET]) and their wild-type littermates (des1$^{+/+}$ mice [WT]) was performed as we have previously described (4).

Animal Studies

Protocols were approved by the Institutional Animal Care and Use Committee of The University of Utah. For the infusion experiments, jugular vein catheters were inserted into 14-week-old male des1 HET and WT mice. Mice were treated with LB1 (1.5 mg/kg/day i.p.) or vehicle (saline) for 3 days (12–14,17). On day 4, conscious unrestrained

mice were infused (5 mL/kg/h × 6 h i.v.) with glycerol or 20% lard oil (15,25). After the infusion, mice were anesthetized with 2–4% isoflurane, and vascular tissue was obtained and used for immunoblotting and vascular function experiments (3,4,23).

For feeding studies, 7-week-old male C57Bl6 mice consumed standard (Con) chow (Research Diets, Inc., New Brunswick, NJ) containing (kilocalories) 10% fat, 70% carbohydrate, and 20% protein (D12450B) or high-fat (HF) chow containing (kilocalories) 45% fat, 35% carbohydrate, and 20% protein (D12451) for 14 weeks (3,4). For the final 14 days, subgroups of Con- and HF-fed mice were treated with vehicle or LB1 (1 mg/kg/day i.p.). At 14 weeks, body composition, glucose tolerance, insulin tolerance, triglycerides, free fatty acids, and blood pressure were assessed as we have previously described (3,4,15,26). Finally, mice were anesthetized with 2–4% isoflurane, perigonadal fat pads were weighed, kidneys were removed for histological analyses, the entire aorta and both iliac arteries were obtained for immunoblotting, and femoral arteries (~150 μm i.d.) were obtained to assess vascular reactivity (3,4,22,23).

Statistics

Data are presented as mean ± SE. Significance was accepted when $P < 0.05$. Comparison of one time point among groups was made using one-way ANOVA. Comparison of multiple time points among groups was made using one-way or two-way repeated-measures ANOVA. Tukey post hoc tests were performed when significant main effects were obtained.

RESULTS

Ceramide Colocalizes With I2PP2A to Promote PP2A Translocation and Interaction With eNOS at the Plasma Membrane

Our earlier results from coimmunoprecipitation experiments using whole-cell lysates indicated that palmitate reduced the association between I2PP2A and PP2A in a ceramide-dependent manner (4), but the initiating event was not examined. To address this, we incubated cells with 500 μmol/L palmitate with or without myriocin (16,27). Palmitate increased ceramide accumulation (Fig. 1*A* and *B*) and PP2A activation (Fig. 1*C* and *D*) in a myriocin-sensitive manner. Sensitivity of immunofluorescence to detect ceramide accumulation and the influence of our treatments on cell viability are shown in Supplementary Fig. 1*A–D*. For determination of whether PP2A activation was sufficient to impair p-eNOS^{Ser1177}, ECs were transfected with either HA-tagged wild-type PP2A-C plasmid (wt) or catalytic site mutant PP2A-C plasmid (mut) and either treated or not treated with 500 μmol/L palmitate. Compared with vehicle, palmitate reduced p-eNOS^{Ser1177} that coimmunoprecipitated with wt but not mut HA-tag PP2A (Fig. 1*E*). EC viability was unaffected (Supplementary Fig. 1*D*).

Next, we determined whether disrupting the inhibitory restraint of I2PP2A on PP2A was sufficient to impair p-eNOS^{Ser1177}. I2PP2A silencing by >60% decreased I2PP2A that coimmunoprecipitated with PP2A, increased PP2A binding with eNOS, and reduced p-eNOS^{Ser1177}–to–total eNOS ratio, relative to results from control (i.e., scrambled siRNA) cells, without altering cell viability (Fig. 1*F–I* and Supplementary Fig. 1*D*).

Additional experiments were performed using confocal microscopy to track fluorescently labeled ceramide, I2PP2A, PP2A, and eNOS in the absence and presence of palmitate. In cells that were incubated with palmitate, ceramide colocalized with I2PP2A (Supplementary Figs. 1*E* and *F* and 2*D* and *E*), I2PP2A dissociated from PP2A (Supplementary Figs. 1*G* and *H* and 2*F* and *G*), and PP2A colocalized with eNOS (Supplementary Figs. 1*I* and *J* and 2*H* and *I*). These effects of palmitate were negated when ceramide biosynthesis was prevented using pharmacological (i.e., myriocin [Supplementary Fig. 1]) and genetic (i.e., Sptlc1 siRNA [Supplementary Fig. 2]) approaches.

The sphingolipid analog FTY720 (Fingolimod; Novartis, Cambridge, MA) was used to gain insight concerning how endogenous ceramide might interact with I2PP2A in ECs to initiate the described events. FTY720 (2-amino-2-[2-(4-octylphenyl)ethyl]propane-1,3-diol) binds to ceramide docking sites on I2PP2A, i.e., K209 and Y122, to an extent that activates PP2A in A549 cells (21,28). For determination of whether FTY720 activates PP2A in our experimental setting, ECs were treated with vehicle, 500 μmol/L palmitate, or 10 μmol/L FTY720 for 3 h. Palmitate and FTY720 decreased p-PP2A^{Tyr307}:PP2A (indicating increased PP2A activity) to the same extent relative to PP2A activity in vehicle-treated cells (Fig. 1*J*), and cell viability was not different among groups (Supplementary Fig. 1*D*). Collectively, results from this set of experiments support the hypothesis that when palmitate elevates ceramide biosynthesis, this sphingolipid binds with I2PP2A and reduces the interaction between PP2A and I2PP2A. When this event occurs, PP2A translocates to the plasma membrane, colocalizes with eNOS, and disrupts the interaction among Akt-Hsp90-eNOS to an extent that impairs NO generation (see below).

Palmitate Suppresses NO Generation in a PP2A-Dependent Manner

Small molecules derived from cantharidin or its demethylated homolog norcantharidin mimic the effects of okadaic acid, a PP2A inhibitor that we and others have used in cell culture models (4,10). The norcantharidin analog LB1 has been synthesized for potential use in cancer treatment and is currently in a phase 1 clinical trial (Lixte Biotechnology Holdings, Inc., East Setauket, NY). LB1 is a potent and specific inhibitor of PP2A activity with relatively low activity on PP1 that can be administered to mice daily for 14 days without pathological evidence of toxicity (12–14). Before use of LB1 in vivo, it was essential to determine its efficacy in the context of our experimental conditions. ECs were treated for 3 h with 500 μmol/L palmitate with or without 0.4–4 μmol/L LB1.

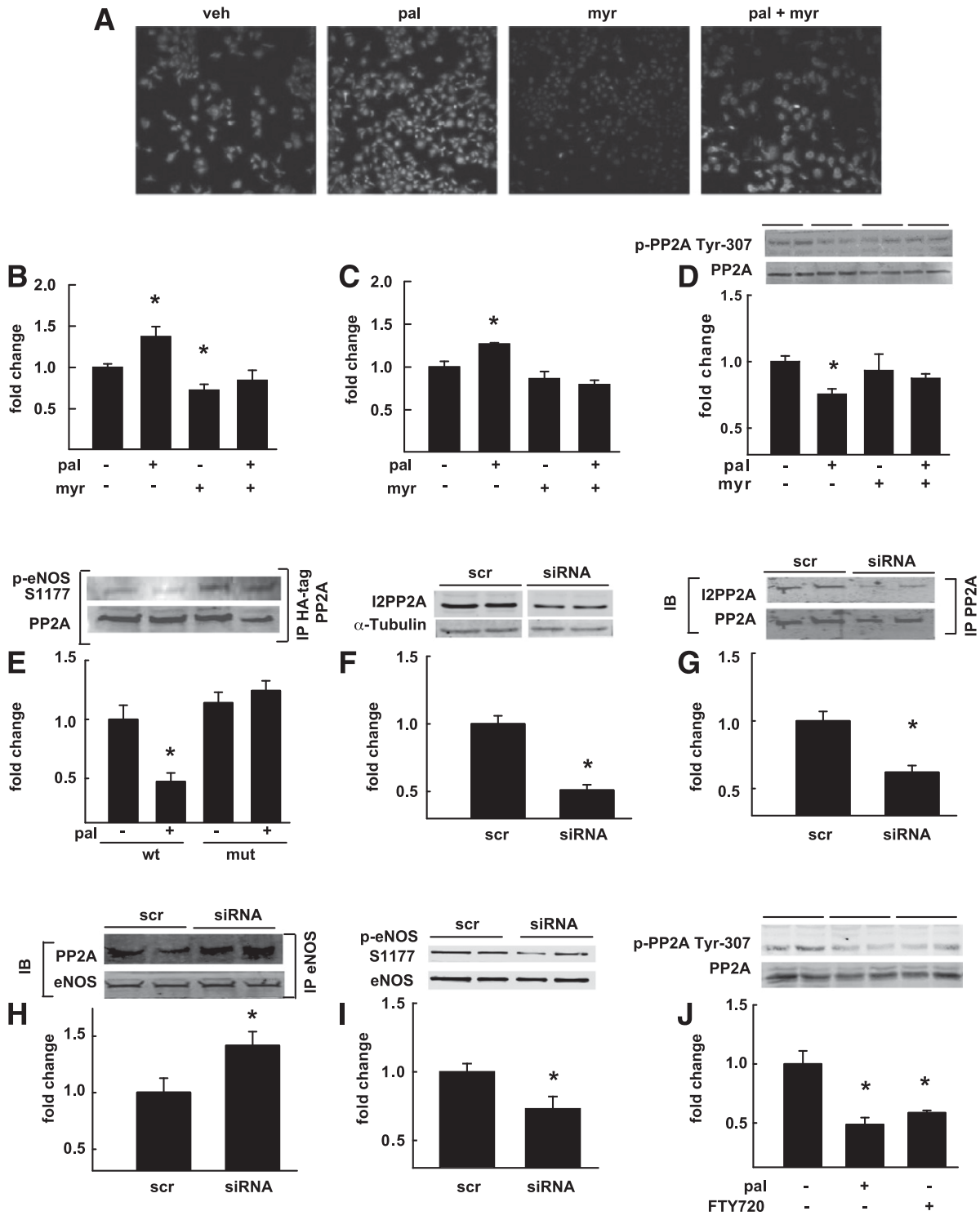

Figure 1— Palmitate-induced ceramide activates PP2A, disrupts PP2A colocalization with I2PP2A, and impairs eNOS^{Ser1177} phosphorylation. Representative images (*A*) and mean data (*B*) indicating that palmitate (pal)-induced ceramide accumulation is prevented by the Ser palmitoyl transferase inhibitor myriocin (myr) (n = 8 per treatment). veh, vehicle. Palmitate-induced increases in PP2A activity (*C*) and reductions in p-PP2A^{Tyr307}:PP2A (*D*) are prevented by myriocin (n = 6–8 per treatment). Palmitate reduced p-eNOS^{Ser1177}:total eNOS after PP2A immunoprecipitation from wt but not mut HA-tag PP2A (*E*). ECs transfected with I2PP2A-targeted siRNA displayed 60% less total protein content (*F*) (n = 6 per treatment), decreased I2PP2A in PP2A immunoprecipitates (*G*) (n = 6 per treatment), increased PP2A after eNOS immunoprecipitation (*H*) (n = 6 per treatment), and decreased p-eNOS^{Ser1177}:total eNOS (*I*) (n = 6 per treatment) vs. ECs transfected with scrambled (scr) siRNA. ECs treated with FTY720 or palmitate exhibited decreased PP2A activity vs. vehicle-treated cells (*J*) (n = 6). For *C*, *D*, *F*, and *J*, each n refers to 1 × 10 cm petri dish. For *E* and *G*–*I*, each n includes 4 × 10 cm petri dishes. Data are mean ± SE. *$P < 0.05$ vs. vehicle-treated ECs, i.e., (-) pal (-) myr (*A*–*D*), (-) pal wt ECs (*E*), scr ECs (*F*, *G*, *H*, and *I*), (-) pal (-) FTY720 (*J*). For *D*–*J*, two representative images are shown above the respective histogram. Additional data pertaining to the above are shown in Supplementary Figs. 1 and 2. IB, immunoblot; ins, insulin; IP, immunoprecipitation; S, serine.

These doses were chosen based on their ability to inhibit Ser/Thr phosphatase activity but not PP1 activity in human glioblastoma multiforme cells (12). LB1 prevented palmitate-induced reductions in p-eNOS^{Ser1177}:eNOS at 4 μmol/L (Fig. 2*A*), and this dose was used in subsequent studies performed in vitro.

As anticipated, palmitate increased PP2A activity in a manner that was sensitive to LB1 treatment (Fig. 2*B* and *C*), and LB1 restored basal and/or insulin-stimulated p-eNOS^{Ser1177}:eNOS (Fig. 2*D*) and NO generation (Fig. 2*E* and *F*) without affecting p-Akt$^{Ser473/T308}$, p-AMPK^{T172}, and p–extracellular signal–regulated kinase 1/2 (Supplementary Fig. 3*A*–*D*). An additional positive eNOS regulatory site, i.e., p-eNOS^{Ser617}, displayed responses to palmitate, insulin, and LB1 that were consistent with p-eNOS^{Ser1177}, whereas the negative regulatory site, i.e., p-eNOS^{T495}, was insensitive to all treatments (Supplementary Fig. 3*E* and *F*). Sensitivity and specificity of our EPR procedures to assess NO generation are respectively displayed in Supplementary Fig. 4. Importantly, palmitate-induced ceramide accumulation was similar regardless of LB1 treatment (Fig. 2*G* and *H*).

PP1 and PP2B are abundantly expressed phosphatases that are activated in tissues from diabetic rats (29), and both can dephosphorylate eNOS^{Ser116} to negatively regulate eNOS enzyme function. For discernment of the contribution from PP1 and/or PP2B to palmitate-induced reductions in p-eNOS^{Ser1177}:eNOS, cells were incubated with or without palmitate, with or without vehicle, with or without 3 μmol/L of the PP1 inhibitor tautomycin, or with or without 100 nmol/L of the PP2B inhibitor cyclosporine. Palmitate-induced reductions in p-eNOS^{Ser1177}:eNOS were refractory to tautomycin and cyclosporine but not LB1 (Supplementary Fig. 5*A* and *B*).

Palmitate Disrupts the Physical Association Among Akt-Hsp90-eNOS in a PP2A-Dependent Manner

We next tested whether LB1 preserves NO bioavailability by preventing palmitate-induced disruptions of the Akt-Hsp90-eNOS complex. ECs were incubated for 3 h with or

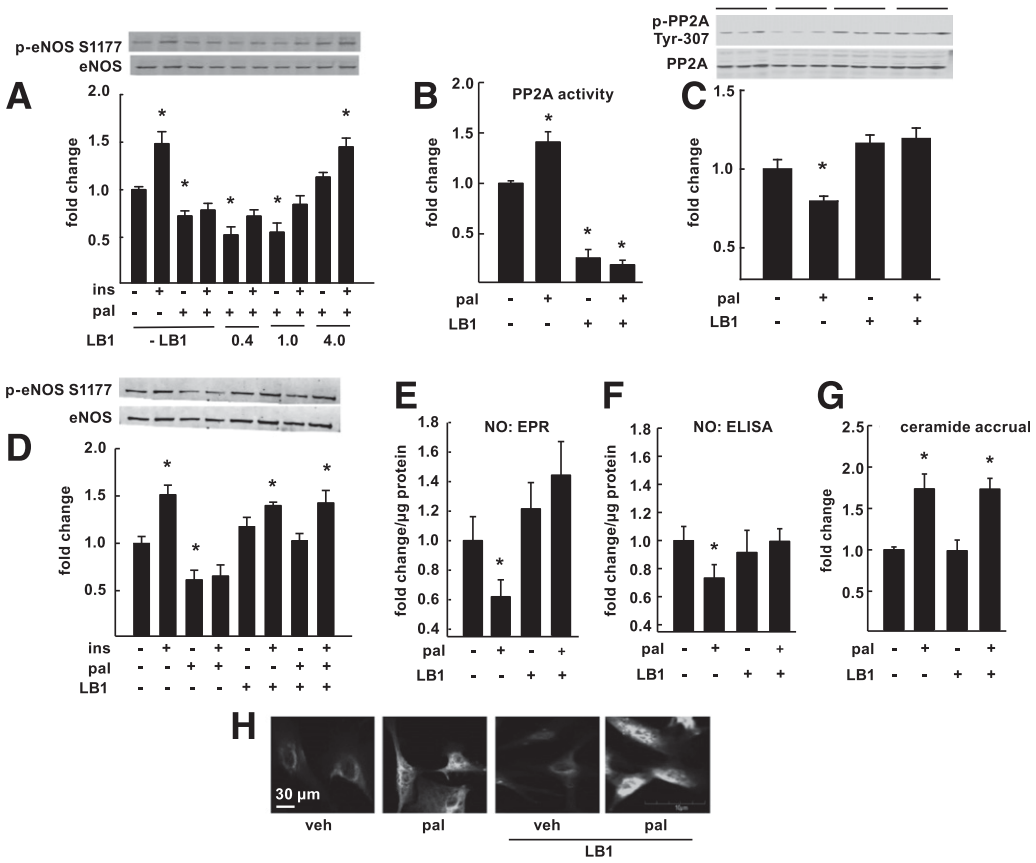

Figure 2—PP2A inhibition prevents palmitate-induced increases in PP2A activity and reductions in NO generation without altering ceramide accumulation. Insulin-stimulated increases in p-eNOS^{Ser1177}:total eNOS are prevented by palmitate (pal) and restored by 4 μmol/L LB1 but not 0.4 or 1 μmol/L LB1 (*A*) (n = 6 per treatment). Palmitate-induced increases in PP2A activity (*B*) (n = 10 per treatment) and reductions in p-PP2A^{Tyr307}:PP2A (*C*) (n = 6 per treatment) were negated by 4 μmol/L LB1. Insulin-induced increases in p-eNOS^{Ser1177}:eNOS were suppressed by palmitate treatment but restored by LB1 treatment (*D*) (n = 6 per treatment). Likewise, palmitate-induced reductions in NO generation assessed via EPR spectroscopy (*E*) (n = 12 per treatment) or ELISA (*F*) (n = 8 per treatment) were restored by LB1 (each n is 3 wells of a 6-well plate). Additional data pertaining to the above are shown in Supplementary Figs. 3–5. Palmitate-induced ceramide accumulation was robust regardless of LB1 treatment (*G* and *H*). Mean data (*G*) and a representative image (*H*) are shown (n = 8). Data are mean ± SE. *P < 0.05 vs. all treatments. ins, insulin; S, serine; Tyr, tyrosine; veh, vehicle.

without 500 μmol/L palmitate and with or without 4 μmol/L LB1, followed by vehicle or insulin treatment for the last 10 min. As expected, palmitate treatment decreased PP2A that coimmunoprecipitated with I2PP2A (Fig. 3*A* and Supplementary Fig. 6*A*) and increased PP2A that associated with eNOS (Fig. 3*B* and Supplementary Fig. 6*B*), but neither effect of palmitate is altered by PP2A inhibition because ceramide accumulation is refractory to LB1 treatment (Fig. 2*G* and *H*). Palmitate suppressed insulin-stimulated p-Akt, Hsp90, and p-eNOS that coimmunoprecipitated with eNOS and was restored by LB1 (Fig. 3*C–E*). Confocal microscopy images of fluorescently labeled eNOS and PP2A (Supplementary Fig. 6*C* and *D*) support the immunoprecipitation/immunoblotting results (Fig. 3*B* and Supplementary Fig. 6*B*) that PP2A associates with eNOS regardless of LB1 treatment, but PP2A activity is inhibited in the presence of LB1 (Fig. 2*B* and *C*).

Results demonstrating that PP2A inhibition using LB1 preserves the interaction among Akt-Hsp90-eNOS were confirmed using a complementary approach. Because eNOS located at the membrane is actively involved in the production of NO (30), we isolated membrane and cytosolic fractions after ECs were exposed to the respective treatments. Fractionation efficacy was confirmed using a subset of ECs from every experiment by the presence of eNOS, insulin receptor, and caveolin-1 in the membrane fraction and GAPDH and actin in the cytosolic fraction (Fig. 4*A*). In the absence of palmitate, insulin increased Akt, p-Akt$^{Ser473/T308}$, Hsp90, and p-eNOS^{Ser1177} at the membrane, while PP2A was unchanged relative to vehicle-treated cells (Fig. 4*B–G*). In the presence of palmitate, PP2A membrane localization was increased and correlated with reduced localization of Akt, p-Akt$^{Ser473/T308}$, Hsp90, and p-eNOS^{Ser1177} under basal and insulin-stimulated conditions. The palmitate-induced impairment in Akt-Hsp90-eNOS association was prevented by myriocin and LB1, implicating contributions from ceramide and PP2A, respectively. Ceramide-mediated palmitate-induced PP2A translocation to the membrane was prevented by myriocin but not by LB1 (Fig. 4*B*). Even though PP2A protein content is increased at the membrane (Fig. 4*B*) and colocalizes with eNOS in palmitate-treated cells (Fig. 3*B* and Supplementary Fig. 6*B–D*) in the presence of LB1, PP2A activity is suppressed in the presence of LB1 (Fig. 2*B* and *C*). The cytosolic levels of I2PP2A, PP2A, and eNOS are shown in Supplementary Fig. 7*A–C*. Collectively, these findings indicate that LB1, a PP2A inhibitor that can be used in vivo, prevents palmitate-induced disruption of the physical association among Akt-Hsp90-eNOS to an extent that preserves NO generation by ECs.

Lard Oil Infusion Disrupts the Physical Interaction Among Akt-Hsp90-eNOS and Evokes Arterial Dysfunction in a Ceramide- and PP2A-Dependent Manner

We next determined whether the efficacy of PP2A inhibition observed in ECs exposed to palmitate could be translated to arteries from mice exposed to lard oil

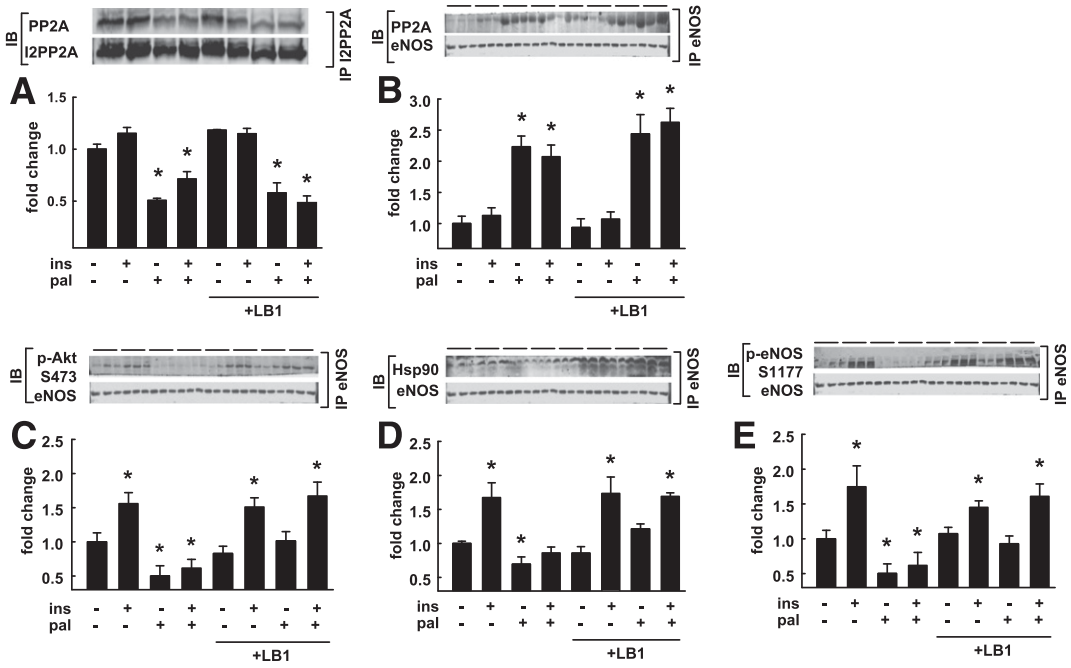

Figure 3—Palmitate-induced PP2A colocalization with eNOS disrupts the physical interaction among eNOS, Akt, and Hsp90. Palmitate (pal) decreased PP2A that coimmunoprecipitated with I2PP2A (*A*) and increased PP2A that associated with eNOS (*B*), but neither effect of pal was altered by PP2A inhibition. Palmitate suppressed insulin (ins)-stimulated p-Akt^{Ser473}, Hsp90, and p-eNOS^{Ser1177} that coimmunoprecipitated with eNOS, and all responses were normalized by LB1 (*C–E*). For experiments *A–E*, n = 6–9 and each n includes 4 × 10 cm petri dishes. For *A*, one representative image is shown above each respective histogram. For *B–E*, three representative images are shown above each respective histogram. Data are mean ± SE. *$P < 0.05$ vs. vehicle, i.e., (-) pal (-) ins. Additional data pertaining to the above are shown in Supplementary Fig. 6. IB, immunoblot; IP, immunoprecipitation; S, serine.

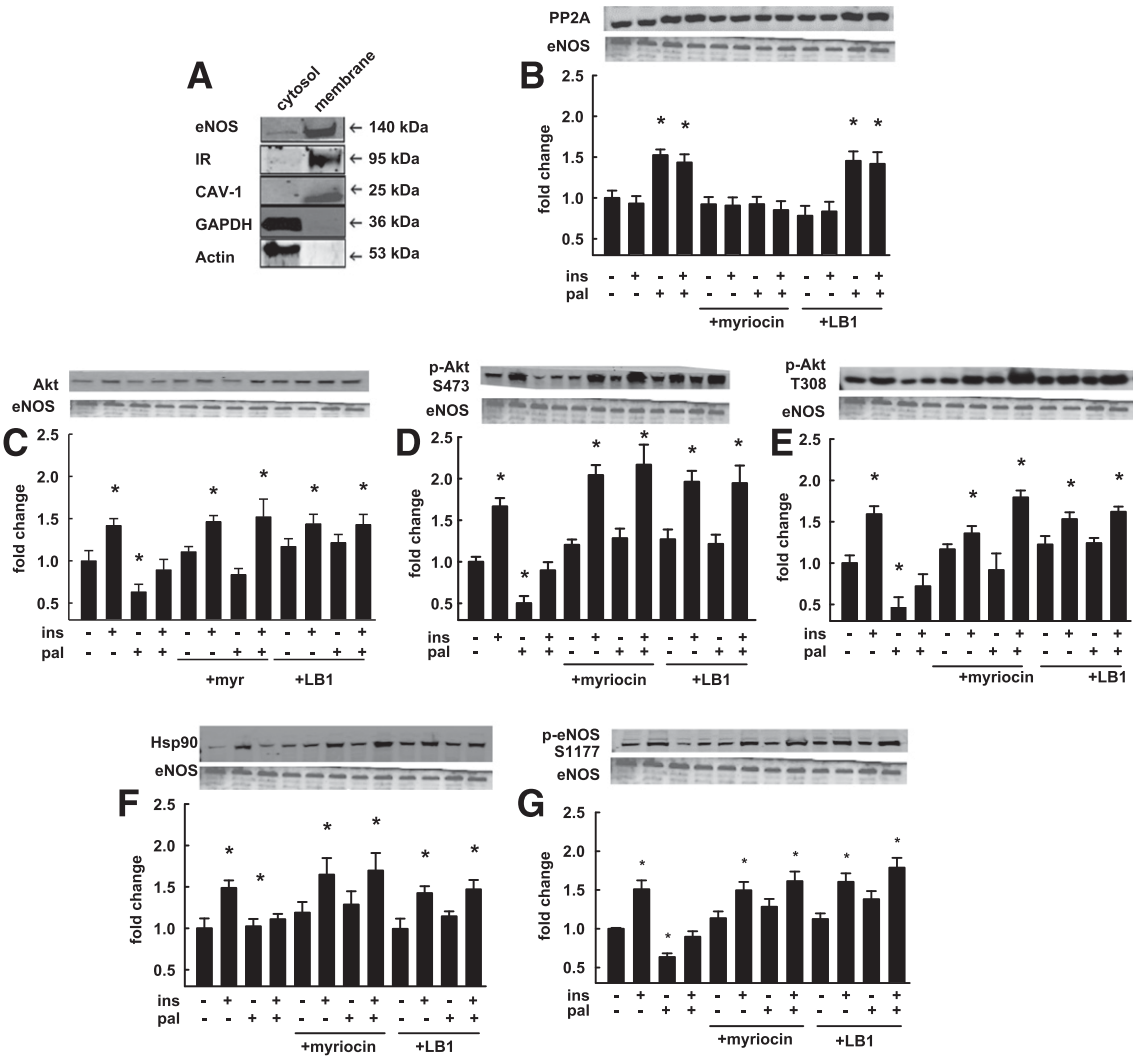

Figure 4—PP2A inhibition prevents palmitate-induced disruption of the Akt-Hsp90-eNOS complex in the membrane fraction. Successful fractionation was verified in a subset of ECs exposed to each treatment (*A*). Compared with vehicle, i.e., (-) pal (-) ins, palmitate (pal) increased PP2A:eNOS at the membrane, a response that was negated by myriocin (myr) but not by LB1 (*B*). Insulin (ins) increased Akt:eNOS (*C*), p-Akt$^{Ser473/T308}$:eNOS (*D* and *E*), Hsp90:eNOS (*F*), and p-eNOS^{Ser1177}:eNOS (*G*). This response was inhibited by palmitate but restored by myriocin and by LB1. For *A–G*, $n = 10$; each n represents 10 × 10 cm petri dishes. Data are mean ± SE. *$P < 0.05$ vs. vehicle-treated cells. Additional data pertaining to the above are shown in Supplementary Fig. 7. CAV-1, caveolin-1; IR, insulin receptor; S, serine; T, threonine.

infusion. To do so, we used des1 HET and WT mice (4,15). Homozygous null mice fail to thrive, but HET animals have a normal life span (15); their body composition, glucose tolerance, serum insulin, triglycerides, and endothelium-dependent and endothelium-independent vascular function are similar to those of WT mice when both consume standard chow; and tissues from HET mice are refractory to ceramide accumulation in response to 3 h of palmitate incubation, 6 h of lard oil infusion, and 14 weeks of high-fat feeding (4,15). After verification of preliminary experiments that vascular PP2A activity is suppressed in mice treated for 3 days with 1.5 mg/kg LB1 versus vehicle (Fig. 5*A* and *B*), conscious and unrestrained WT and HET mice were infused (intravenously) with glycerol for 6 h after treatment with vehicle for 3 days. Because responses (e.g., immunoblotting, vascular reactivity) to glycerol infusion after vehicle treatment were similar in WT and HET mice, data were combined and are referred to as control (CON) in Fig. 5*C–J*. Compared with results in control mice, 20% lard oil infusion to WT mice pretreated with vehicle for 3 days increased PP2A activity (Fig. 5*C*) and C16:0 (78%) and C18:0 (99%) ceramides, the ceramide species most associated with impaired insulin action (31,32). Immunoblotting performed after eNOS immunoprecipitation showed that lard oil infusion increased the amount of PP2A that coimmunoprecipitated with eNOS in vessels from WT mice pretreated with vehicle and less Akt and Hsp90 was associated with eNOS relative to results from control mice (Fig. 5*D–F*). In HET mice infused with lard oil after 3 days of vehicle treatment, ceramide biosynthesis and PP2A activity did not increase and PP2A did not associate with eNOS, Akt, and Hsp90 in eNOS

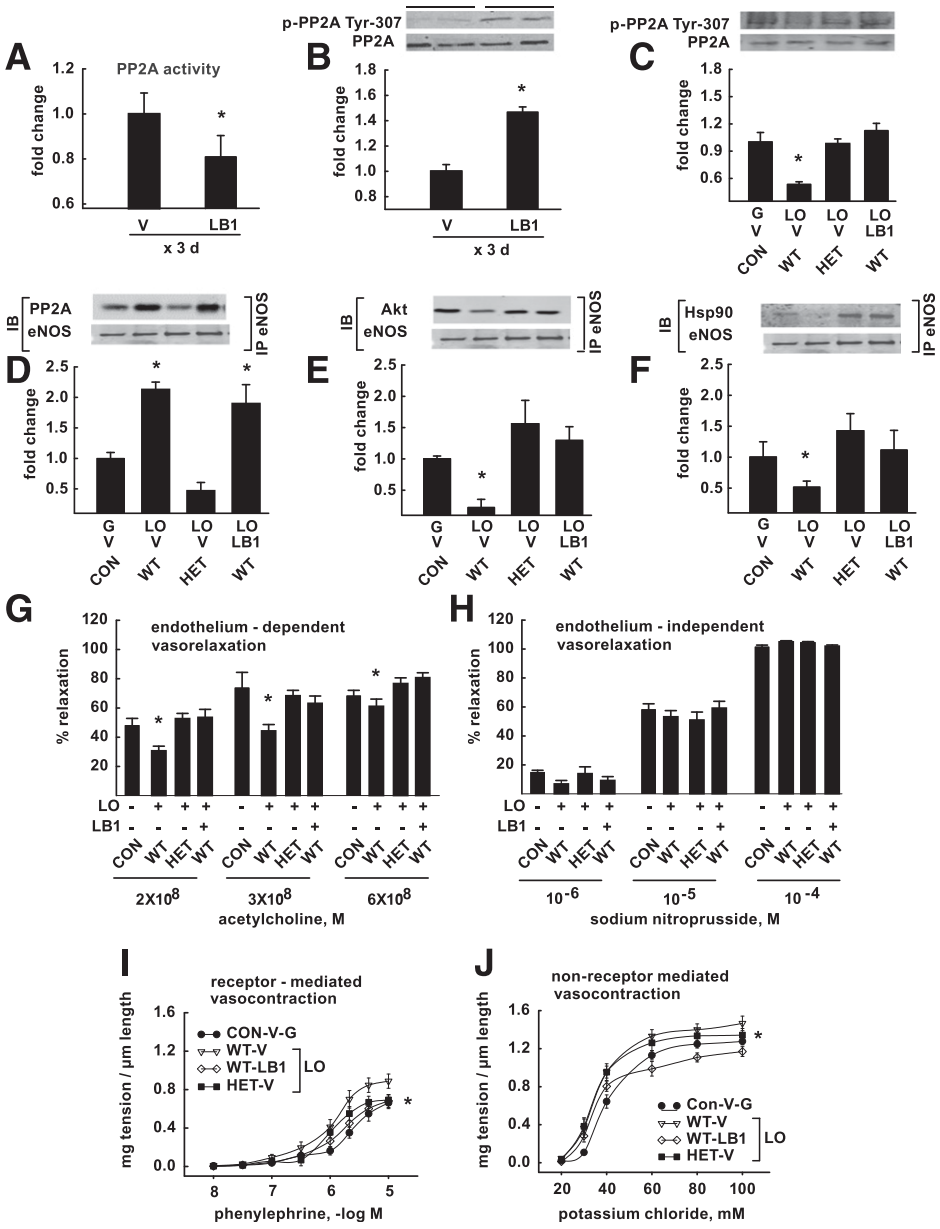

Figure 5—Lard oil increases PP2A activity; disrupts interactions among Akt, Hsp90, and eNOS in the vasculature; and precipitates arterial dysfunction, each of which is prevented by ceramide synthesis inhibition and PP2A inhibition. Arteries from C57Bl6 mice treated for 3 days with 1.5 mg/kg LB1 exhibit reduced PP2A activity (*A*) and increased p-PP2A^{Tyr307}:PP2A (*B*) vs. arteries from mice treated with vehicle (V). Compared with arteries from des1$^{+/+}$ (WT) and des1$^{+/-}$ (HET) mice pretreated for 3 days with vehicle followed by 6 h of glycerol (G) infusion (collectively referred to as CON), p-PP2A^{Tyr307}:PP2A was lower in liver from WT mice pretreated with vehicle and subsequently infused for 6 h with lard oil (LO) (*C*). The lard oil–induced reduction in vascular PP2A^{Tyr307}:PP2A is attenuated in HET mice pretreated with vehicle and in WT mice pretreated with LB1. Aorta/iliac homogenates were prepared as appropriate to immunoblot for PP2A, Akt, and Hsp90 after eNOS immunoprecipitation (*D–F*). Compared with arteries from control mice, LO infusion to WT mice pretreated with vehicle increased PP2A association with eNOS (*D*), while Akt (*E*) and Hsp90 (*F*) that coimmunoprecipitated with eNOS were reduced. The LO-induced disruption of the Akt-Hsp90-eNOS complex was prevented in HET mice pretreated with vehicle (implicating ceramide) and in WT mice pretreated with LB1 (implicating PP2A). Vascular function was assessed in femoral artery segments from the same animals. Compared with arteries from control mice, endothelium-dependent vasorelaxation was impaired, and receptor- and non–receptor-mediated vasocontraction was exaggerated in vessels from WT mice pretreated with vehicle and infused for 6 h with LO (*G–I*). Indices of vascular dysfunction were attenuated in HET mice pretreated with vehicle (implicating ceramide) and in WT mice pretreated with LB1 (implicating PP2A). Because no differences were observed among groups for endothelium-independent vasorelaxation (*J*), the LO-induced defect observed in WT mice pretreated with vehicle likely was specific to the endothelium. For *A–C*, n = 2–3 mice per group. For *D–F*, n = 5–7 mice per group. For *G–J*, n = 5–7 mice per group, 2–4 vessels per mouse. Data are mean ± SE. *$P < 0.05$ vs. all. d, days; IB, immunoblot; IP, immunoprecipitation.

immunoprecipitates (Fig. 5*D–F*). PP2A activity did not increase in WT mice infused with lard oil that were pretreated with LB1, and despite its persistent association with eNOS, Akt, and Hsp90, eNOS phosphorylation was not reduced.

Vascular reactivity was assessed in femoral artery segments from the same experimental groups. Characteristics of the arteries are shown in Supplementary Table 2. Compared with results in control mice, endothelium-dependent vasorelaxation was impaired (Fig. 5*G*) and receptor-mediated (Fig. 5*I*) and non–receptor-mediated vasocontraction were exaggerated (Fig. 5*J*) in arteries from WT mice infused with lard oil that were pretreated with vehicle. Notably, lard oil–induced dysfunction was less severe in vessels from HET mice pretreated with vehicle (implicating ceramide) and in arteries from WT mice pretreated with LB1 (implicating PP2A). Because sodium nitroprusside–evoked vasorelaxation was similar among groups (Fig. 5*H*), the lard oil–induced defect observed in vessels from WT mice treated with vehicle likely was specific to the endothelium. These findings indicate that lard oil–induced, ceramide-mediated PP2A activation in vivo contributes to endothelial dysfunction.

PP2A Inhibition Restores Physical Interactions Among Akt-Hsp90-eNOS and Prevents Systemic Hypertension and Arterial Dysfunction in Obese Mice

Because 1.0 but not 0.5 mg/kg LB1 reduced vascular PP2A activity when given for 21 days (Fig. 6*A*), this dose of LB1 (or vehicle) was given to Con- and HF-fed mice for the last 14 days of a 14-week protocol to test whether endothelial dysfunction and hypertension evoked by fat feeding is attenuated by PP2A inhibition. Relative to Con-fed mice, vascular PP2A activity increased in HF-fed mice treated with vehicle (HF-V) but not HF-fed mice treated with LB1 (HF-LB1) (Fig. 6*B*). The impact of fat feeding on body mass, fat mass, glucose tolerance, insulin tolerance, triglycerides, and FFAs (Fig. 6*C–I* and Supplementary Fig. 8) was similar regardless of LB1 treatment, but hypertension was prevented by PP2A inhibition (Fig. 7*A*).

Lower basal p-eNOS^{Ser1177} was observed in arteries from HF-V mice (Fig. 7*B*), but Akt, AMPK, and extracellular signal–regulated kinase 1/2 expression or phosphorylation

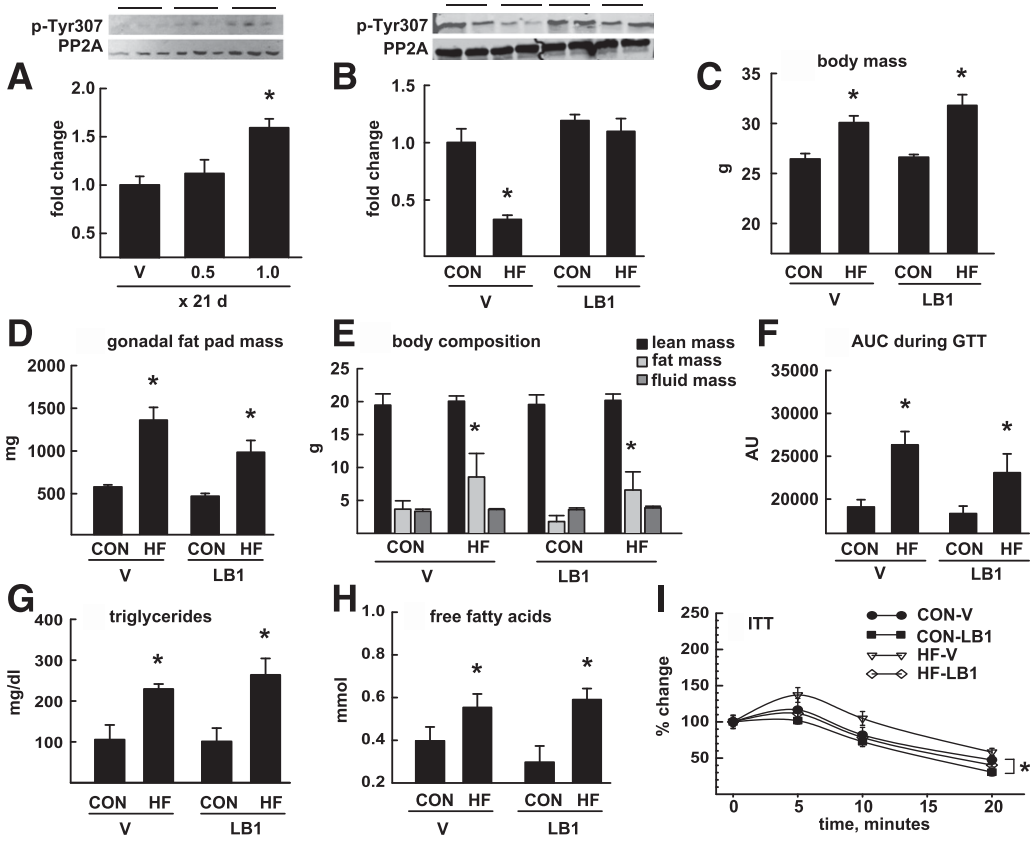

Figure 6—Metabolic phenotype of fat-fed mice with or without PP2A inhibition. Arteries from mice treated (intraperitoneally) with 1.0 mg/kg/day LB1 ×21 days vs. 0.5 mg/kg/day exhibited increased p-PP2A^{Tyr307}:PP2A vs. arteries from mice treated with vehicle (V) (*A*). Mice that consumed standard (Con) or high-fat (HF) chow for 14 weeks were treated with vehicle or LB1 for the final 14 days. p-PP2A^{Tyr307}:PP2A was lower in arteries from HF-V mice vs. all other groups (*B*). Increases in body mass (*C*), gonadal fat pad mass (*D*), whole-body fat mass (*E*), area under the curve (AUC) during the glucose tolerance test (GTT) (*F*), triglycerides (*G*), and FFAs (*H*) and reductions in circulating glucose upon insulin stimulation (*I*) were similar in HF-fed mice regardless of LB1 treatment. Glucose levels measured at 20 min of the insulin tolerance test (ITT) were lower in Con-fed mice treated with LB1 vs. vehicle. Additional data pertaining to the above are shown in Supplementary Fig. 8. For *A* and *B*, $n = 3$ mice per group. For *C–I*, $n = 8–10$ mice per group. Data are mean ± SE. *$P < 0.05$ vs. all. AU, arbitrary units; d, days; Tyr, tyrosine.

was similar among groups (Supplementary Table 4). Compared with arteries from chow-fed mice treated with vehicle (saline) for the final 14 days (Con-V animals), PP2A that coimmunoprecipitated with eNOS was increased, whereas Akt and Hsp90 association with eNOS was reduced in arteries from mice fed high-fat chow that were treated with vehicle (HF-V) for the final 14 days (Fig. 7*C–E*). The reduced p-eNOS^{Ser1177} and lower content of Akt and Hsp90 in the eNOS complex were normalized in HF-fed mice treated with LB1, despite persistent association of PP2A with eNOS.

Relative to animals on a control diet, in femoral arteries from HF-V mice, endothelium-dependent vasorelaxation was impaired (Fig. 8*A*) but was normalized by LB1 treatment. Endothelium-independent vasorelaxation was similar in all groups (Fig. 8*B*), and receptor- and non–receptor-mediated vasocontraction were exaggerated by HF feeding and restored by LB1 (Fig. 8*C* and *D*). Differences in endothelium-dependent vasorelaxation and receptor-mediated vasocontraction were eliminated in all groups after pretreatment with N^G-monomethyl-L-arginine salt (Fig. 8*E* and *F*). Characteristics of femoral artery segments used to assess vascular function are shown in Supplementary Table 3. A schematic representation of our findings is shown in Fig. 8*G*.

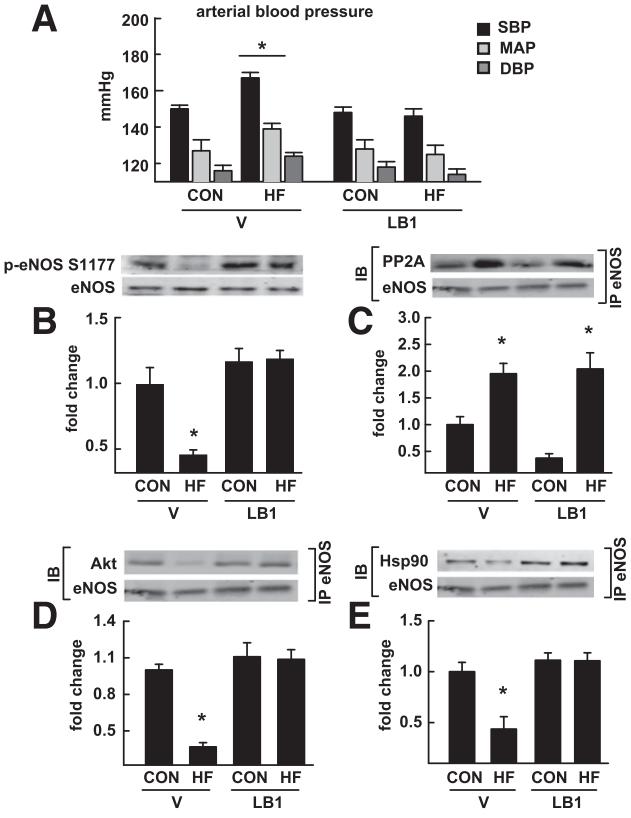

Figure 7—Systemic blood pressure is elevated and vascular Akt-Hsp90-eNOS association is disrupted in obese vs. lean mice, each of which is prevented by PP2A inhibition. Elevations in arterial blood pressure evoked by fat feeding were negated in obese mice treated with LB1 (*A*). Heart rate (bpm) during conscious blood pressure determinations was not different among groups, i.e., CON-V, 739 ± 13; HF-V, 765 ± 12; CON-LB1, 734 ± 18; HF-LB1, 742 ± 12. p-eNOS^{Ser1177}:eNOS was lower in arterial homogenates from HF-V mice vs. all other groups (*B*). Using the same samples, an IP for eNOS was performed, followed by IB for PP2A, Akt, and Hsp90 (*C–E*). Consistent with reduced p-eNOS^{Ser1177}:eNOS in arteries from HF-V mice vs. all groups, PP2A was elevated in the eNOS complex (*C*), while Akt (*D*) and Hsp90 (*E*) were reduced. These changes were normalized in obese mice treated with LB1 for the final 14 days of fat feeding, except that PP2A remained in the eNOS complex. $n = 6$ mice per group. Data are mean ± SE. *$P < 0.05$ vs. all. DBP, diastolic blood pressure; IB, immunoblot; IP, immunoprecipitation; MAP, mean arterial blood pressure; SBP, systolic blood pressure; S, serine; V, treatment with saline for final 14 days.

DISCUSSION

Protein phosphatases coordinately regulate cellular metabolism but may become dysregulated in pathophysiological situations (33,34). PP2A is highly conserved from yeast to humans, and evidence exists that hyperactivation of PP2A has the potential to contribute importantly to ceramide-mediated vascular dysfunction (4,10,11,33–35).

We sought to discern a mechanism whereby ceramide initiates PP2A colocalization with eNOS that we (4) and others (11) have reported. I2PP2A restrains PP2A under physiological situations (36,37). Data obtained using a variety of reagents and approaches, including *1*) the sphingolipid analog FTY720, *2*) I2PP2A knockdown, *3*) subcellular localization via confocal microscopy of fluorescently labeled proteins, *4*) immunoprecipitation and immunoblotting, *5*) cellular fractionation, and *6*) a catalytically inactive PP2A mutant, yield congruent results that provide important insight into how this restraint is disrupted and the functional consequences that ensue in the context of lipotoxicity. Collectively, when endogenous ceramide levels increase in response to palmitate, this sphingolipid binds to I2PP2A in the cytosol, the restraint that I2PP2A normally confers upon PP2A is disrupted, the association between PP2A and eNOS at the cell membrane and in the perinuclear space is increased, and p-eNOS^{Ser1177} and NO generation are impaired.

An important posttranslational modification of eNOS dysregulated in obesity, which likely contributes to arterial dysfunction, is suppressed p-eNOS^{Ser1177} (3,4,10). Protein kinases and phosphatases, respectively, add and remove phosphate groups from their target proteins (30,33). In our earlier investigations, reduced p-eNOS^{Ser1177} and NO generation in ECs treated with palmitate and in arteries from obese mice were observed but upstream kinases known to modulate eNOS function were intact (3,4). These findings prompted us to explore the role that dysregulated phosphatase signaling might play in this regard and to provide mechanistic insights into earlier observations that implicated PP2A hyperactivation in contributing to arterial dysfunction. For example, suppressed endothelial glutathione concentrations were described in aging rats leading to activation of neutral sphingomyelinases that increased vascular ceramide and PP2A activity, thereby disrupting the balance between p-eNOS^{Ser1177} and p-eNOS^{T495} (35). Although arterial dysfunction

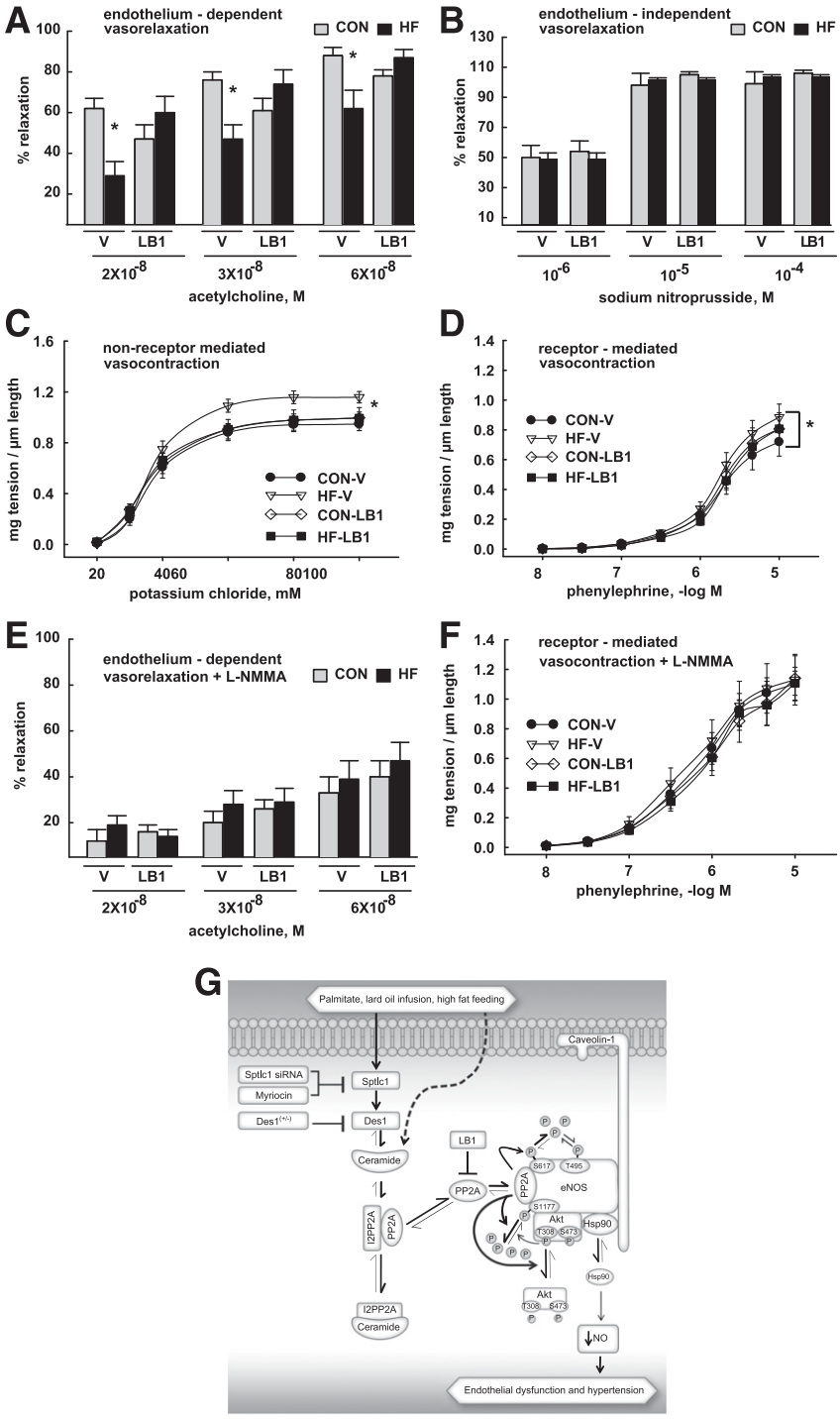

Figure 8—Vascular dysfunction exists in obese vs. lean mice, which is prevented by PP2A inhibition. Vascular function was assessed in femoral artery segments from the same mice used in Fig. 7. Endothelium-dependent vasorelaxation was impaired in arteries from HF-V mice vs. all groups (*A*), while endothelium-independent vasorelaxation (*B*) was similar among animals. Non–receptor-mediated vasoconstraction (*C*) and receptor-mediated vasocontraction (*D*) were greater in arteries from HF-V mice vs. all groups but normalized by PP2A inhibition. Impaired responses to acetylcholine (*A*) and increased responsiveness to phenylephrine (*D*) observed in arteries from HF-V mice were equalized among groups by prior treatment with N^G-monomethyl-L-arginine salt (L-NMMA) (*E* and *F*, respectively). For *A*–*F*, n = 8–10 mice per group, 2–4 vessel segments per mouse. Data are mean ± SE. **P* < 0.05 vs. Con-fed mice. A schematic summary of our findings is presented in *G*. Palmitate, lard oil infusion, and fat feeding elevate cellular ceramide biosynthesis. Ceramide binds I2PP2A, the restraint that I2PP2A confers upon PP2A is inhibited, and PP2A that translocates to the membrane disrupts interactions among Akt, Hsp90, and eNOS to an extent that NO generation and vascular function are impaired. All effects can be prevented by pharmacological (myriocin) and genetic (Sptlc1 siRNA; des1$^{+/-}$ mice) manipulations that inhibit ceramide biosynthesis, and all effects (except for PP2A translocation to the eNOS complex) can be prevented by mutation of the catalytic site on PP2A and by PP2A inhibition using LB1. These results indicate that PP2A activation contributes to vascular dysfunction in vivo. P, phosphorylation; S, serine; T, threonine; V, treatment with saline for final 14 days.

observed in old versus young rats was reversed in vitro by neutral sphingomyelinase inhibition, a direct effect of PP2A was not evaluated. Wu et al. (10) examined the hypothesis that PP2A-mediated dephosphorylation of p-AMPK^{T172} was responsible for impaired p-eNOS^{Ser1177} in vessels from mice fed a palmitate-rich versus oleate-rich high-fat diet. Interestingly, p-AMPK^{T172} and p-eNOS^{Ser1177} improved in vessels from mice fed a palmitate-rich high-fat diet 48 h after retro-orbital treatment with PP2A siRNA, but the functional consequences of this biochemical modification of eNOS were not assessed. Most recently, it was reported that vascular endothelial growth factor–induced p-eNOS^{Ser1177} and NO generation were suppressed in ECs that were coincubated with palmitate in a manner that was sensitive to ceramide biosynthesis (myriocin) and PP2A (okadaic acid) inhibition (11), confirming results we reported earlier using another eNOS agonist, i.e., insulin (4). These authors extended their in vitro findings by showing that growth factor–induced NO production was blunted in arteries from wild-type but not Sptlc2 haploinsufficient mice that consumed high-fat chow for 2.5 weeks, clarifying the importance of ceramide in this regard, but the independent contribution from PP2A activation to NO-mediated arterial function was not assessed. In an earlier study, we used pharmacological and genetic approaches that limit ceramide accumulation to show that ceramide contributes importantly to endothelial dysfunction and hypertension that exist in the context of diet-induced obesity (4). Again, even though coimmunoprecipitation of PP2A with eNOS was increased in arteries from fat-fed mice in a ceramide-dependent manner, the independent contribution from PP2A activation to vascular dysfunction was not explored.

While solid rationale exists to determine whether hyperactivation of PP2A impairs blood vessel function, concerns regarding cytotoxicity for cantharidin-derived compounds, efficacy for norcantharidin-derived compounds, and target specificity for genetic knockout models have precluded exploration of this hypothesis (17,38,39). However, relatively recent investigations of PP2A activation in the context of cancer chemotherapy using mice (12–14) and hepatic insulin resistance using rats (17) reported that 3- to 21-day treatment with the norcantharidin analog LB1 was safe and efficacious. We first demonstrated that LB1 prevented palmitate-induced PP2A activation, restored basal and insulin-stimulated p-eNOS^{Ser1177} and NO production, and did not influence upstream kinase signaling to eNOS or ceramide accumulation. Next, multiple approaches established that the PP2A disruption of Akt-Hsp90-eNOS interactions correlated with impaired p-eNOS^{Ser1177} and NO production, and this could be prevented by PP2A inhibition or a PP2A mutant with decreased catalytic activity. Third, after documenting that lard oil infusion increases vascular PP2A activity; disrupts the physical interactions among Akt, Hsp90, and eNOS in the vasculature; and precipitates endothelium-dependent dysfunction, we showed that these responses could be prevented by inhibiting ceramide biosynthesis (i.e., HET mice) or limiting PP2A activation (i.e., LB1-treated mice). Finally, dysregulation of vascular Akt-Hsp90-eNOS signaling, endothelial dysfunction, and systemic hypertension was normalized when fat-fed mice were treated with LB1. Collectively, these findings indicate that PP2A activation evoked by palmitate in ECs and by lard oil infusion and fat feeding in mice has deleterious consequences on endothelial function and that pharmacological inhibition of PP2A may reverse lipotoxicity-induced vascular dysfunction.

Vascular PP2A activity is increased in pathologies associated with suppressed p-eNOS^{Ser1177} and compromised endothelial function (4,10,35,40). Our results suggest strongly that therapeutic strategies targeted to lower ceramide-mediated PP2A activation might be beneficial in attenuating vascular complications associated with obesity, type 2 diabetes, and insulin resistance.

Acknowledgments. The authors thank John S. Kovach (Lixte Biotechnology Holdings, Inc.) for the kind donation of LB1, Diana Lim for all of the figures, Dr. Charles Murtaugh for his helpful comments concerning confocal microscopy, Dr. Jared Rutter for comments and suggestions throughout the course of this study, and Drs. Todd Miller and Besim Ogretman for the PP2A–C and I2PP2A mutant plasmids, respectively.

Funding. This work was funded, in part, by the American Diabetes Association (1-12-BS-208, ADA 7-08-RA-164), the National Institutes of Health (NIH) (2R15HL091493), and Seed Grants from The University of Utah (UU) Office of the Vice President for Research and the UU College of Health to J.D.S.; American Heart Association Grant 12BGIA8910006 (to W.L.H.); and NIH RO1 DK092065 (to E.D.A.). Student support was provided by the American Physiological Society (APS) Undergraduate Research Program (T.R. and J.K.N), APS Undergraduate Research Excellence Fellowship Program (T.R.), APS STEP-UP Program (Emma Uzoigwe), the American Heart Association Western States Affiliate Undergraduate Student Summer Research Program (T.R., A.R., X.W., Molly Morton), the ADA Minority Undergraduate Internship Program (Emma Uzoigwe), the Science Without Borders Program of the Government of Brazil (Paula Fernandes, Juliana Goncalves, and Izabela Carvelho), the Native American Research Internship Program (Wallita Begay and Alex Kivimaki), the UU Undergraduate Research Opportunities Program (T.R., A.R., X.W., J.K.N., M.L.W., L.D., R.G., E.J., D.M., D.K., Lyman Wood, Quinn Shelton, and Preeya Prakash), and an NIH Short-Term Training Students in Health Professional Schools Grant T35 HL007744 to Erik Ostler (Dr. J. Kaplan, PI).

Duality of Interest. No potential conflicts of interest relevant to this article were reported.

Author Contributions. L.P.B. researched data, assisted with experimental design, and wrote the manuscript. L.P.B., T.R., Y.L., A.R., J.K.N., M.L.W., and R.M. performed cell culture experiments. X.W., L.D., R.G., E.J., D.M., D.K., and J.D.S. performed vascular reactivity experiments. L.P.B., L.D., D.K., D.J., P.V.A.B., W.L.H., and J.D.S. assisted with metabolic characterization and/or blood pressure evaluations. V.R. facilitated the EPR assessments of NO. T.R., A.R., X.W., J.K.N., L.D., R.G., E.J., D.M., R.M., and D.K. researched data as UU undergraduate students. L.P.B., S.A.S., P.V.A.B., W.L.H., Q.-J.Z., and E.D.A. reviewed and edited the manuscript. E.D.A. and J.D.S. conceived the study and oversaw its design and implementation. J.D.S. researched data and wrote, reviewed, and edited the manuscript. J.D.S. is the guarantor of this work and, as such, had full access to all the data in the study and takes responsibility for the integrity of the data and the accuracy of the data analysis.

Prior Presentation. Parts of this study were presented in abstract form at the 73rd Scientific Sessions of the American Diabetes Association, Chicago, IL,

21–25 June 2013; Experimental Biology 2012, San Diego, CA, 21–25 April 2012; Experimental Biology 2013, Boston, MA, 20–24 April 2013; Experimental Biology 2014, San Diego, CA, 26–30 April 2014; the 74th Scientific Sessions of the American Diabetes Association, San Francisco, CA, 13–17 June 2014; Experimental Biology 2015, Boston, MA, 28 March–1 April 2015; and the Cardiovascular Forum for Promoting Centers of Excellence and Young Investigators, Louisville, KY, 15–17 August 2013.

References

1. Triggle CR, Ding H. A review of endothelial dysfunction in diabetes: a focus on the contribution of a dysfunctional eNOS. J Am Soc Hypertens 2010;4:102–115
2. Symons JD, Abel ED. Lipotoxicity contributes to endothelial dysfunction: a focus on the contribution from ceramide. Rev Endocr Metab Disord 2013;14:59–68
3. Symons JD, McMillin SL, Riehle C, et al. Contribution of insulin and Akt1 signaling to endothelial nitric oxide synthase in the regulation of endothelial function and blood pressure. Circ Res 2009;104:1085–1094
4. Zhang QJ, Holland WL, Wilson L, et al. Ceramide mediates vascular dysfunction in diet-induced obesity by PP2A-mediated dephosphorylation of the eNOS-Akt complex. Diabetes 2012;61:1848–1859
5. Tripathy D, Mohanty P, Dhindsa S, et al. Elevation of free fatty acids induces inflammation and impairs vascular reactivity in healthy subjects. Diabetes 2003;52:2882–2887
6. Steinberg HO, Tarshoby M, Monestel R, et al. Elevated circulating free fatty acid levels impair endothelium-dependent vasodilation. J Clin Invest 1997;100:1230–1239
7. Steinberg HO, Chaker H, Leaming R, Johnson A, Brechtel G, Baron AD. Obesity/insulin resistance is associated with endothelial dysfunction. Implications for the syndrome of insulin resistance. J Clin Invest 1996;97:2601–2610
8. Summers SA. Sphingolipids and insulin resistance: the five Ws. Curr Opin Lipidol 2010;21:128–135
9. Holland WL, Summers SA. Sphingolipids, insulin resistance, and metabolic disease: new insights from in vivo manipulation of sphingolipid metabolism. Endocr Rev 2008;29:381–402
10. Wu Y, Song P, Xu J, Zhang M, Zou MH. Activation of protein phosphatase 2A by palmitate inhibits AMP-activated protein kinase. J Biol Chem 2007;282:9777–9788
11. Mehra VC, Jackson E, Zhang XM, et al. Ceramide-activated phosphatase mediates fatty acid-induced endothelial VEGF resistance and impaired angiogenesis. Am J Pathol 2014;184:1562–1576
12. Lu J, Kovach JS, Johnson F, et al. Inhibition of serine/threonine phosphatase PP2A enhances cancer chemotherapy by blocking DNA damage induced defense mechanisms. Proc Natl Acad Sci U S A 2009;106:11697–11702
13. Lu J, Zhuang Z, Song DK, et al. The effect of a PP2A inhibitor on the nuclear receptor corepressor pathway in glioma. J Neurosurg 2010;113:225–233
14. Martiniova L, Lu J, Chiang J, et al. Pharmacologic modulation of serine/threonine phosphorylation highly sensitizes PHEO in a MPC cell and mouse model to conventional chemotherapy. PLoS One 2011;6:e14678
15. Holland WL, Brozinick JT, Wang LP, et al. Inhibition of ceramide synthesis ameliorates glucocorticoid-, saturated-fat-, and obesity-induced insulin resistance. Cell Metab 2007;5:167–179
16. Miyake Y, Kozutsumi Y, Nakamura S, Fujita T, Kawasaki T. Serine palmitoyltransferase is the primary target of a sphingosine-like immunosuppressant, ISP-1/myriocin. Biochem Biophys Res Commun 1995;211:396–403
17. Galbo T, Perry RJ, Nishimura E, Samuel VT, Quistorff B, Shulman GI. PP2A inhibition results in hepatic insulin resistance despite Akt2 activation. Aging (Albany, NY) 2013;5:770–781
18. Harris MB, Ju H, Venema VJ, et al. Reciprocal phosphorylation and regulation of endothelial nitric-oxide synthase in response to bradykinin stimulation. J Biol Chem 2001;276:16587–16591
19. Yang D, Li Q, So I, et al. IRBIT governs epithelial secretion in mice by antagonizing the WNK/SPAK kinase pathway. J Clin Invest 2011;121:956–965
20. Chung H, Brautigan DL. Protein phosphatase 2A suppresses MAP kinase signalling and ectopic protein expression. Cell Signal 1999;11:575–580
21. Mukhopadhyay A, Saddoughi SA, Song P, et al. Direct interaction between the inhibitor 2 and ceramide via sphingolipid-protein binding is involved in the regulation of protein phosphatase 2A activity and signaling. FASEB J 2009;23:751–763
22. Zhang QJ, McMillin SL, Tanner JM, Palionyte M, Abel ED, Symons JD. Endothelial nitric oxide synthase phosphorylation in treadmill-running mice: role of vascular signalling kinases. J Physiol 2009;587:3911–3920
23. Symons JD, Hu P, Yang Y, et al. Knockout of insulin receptors in cardiomyocytes attenuates coronary arterial dysfunction induced by pressure overload. Am J Physiol Heart Circ Physiol 2011;300:H374–H381
24. Rockstroh M, Muller S, Jende C, Kerzhner A, Bergen M, Tomm J. Cell fractionation - an important tool for compartment proteomics. J Integr OMICS 2011;01:135–143
25. Stein DT, Stevenson BE, Chester MW, et al. The insulinotropic potency of fatty acids is influenced profoundly by their chain length and degree of saturation. J Clin Invest 1997;100:398–403
26. Babu PV, Si H, Fu Z, Zhen W, Liu D. Genistein prevents hyperglycemia-induced monocyte adhesion to human aortic endothelial cells through preservation of the cAMP signaling pathway and ameliorates vascular inflammation in obese diabetic mice. J Nutr 2012;142:724–730
27. Wadsworth JM, Clarke DJ, McMahon SA, et al. The chemical basis of serine palmitoyltransferase inhibition by myriocin. J Am Chem Soc 2013;135:14276–14285
28. Saddoughi SA, Gencer S, Peterson YK, et al. Sphingosine analogue drug FTY720 targets I2PP2A/SET and mediates lung tumour suppression via activation of PP2A-RIPK1-dependent necroptosis. EMBO Mol Med 2013;5:105–121
29. Foulkes JG, Jefferson LS. Protein phosphatase-1 and -2A activities in heart, liver, and skeletal muscle extracts from control and diabetic rats. Diabetes 1984;33:576–579
30. Wei Q, Xia Y. Proteasome inhibition down-regulates endothelial nitric-oxide synthase phosphorylation and function. J Biol Chem 2006;281:21652–21659
31. Raichur S, Wang ST, Chan PW, et al. CerS2 haploinsufficiency inhibits β-oxidation and confers susceptibility to diet-induced steatohepatitis and insulin resistance. Cell Metab 2014;20:687–695
32. Turpin SM, Nicholls HT, Willmes DM, et al. Obesity-induced CerS6-dependent C16:0 ceramide production promotes weight gain and glucose intolerance. Cell Metab 2014;20:678–686
33. Shi Y. Serine/threonine phosphatases: mechanism through structure. Cell 2009;139:468–484
34. Kowluru A, Matti A. Hyperactivation of protein phosphatase 2A in models of glucolipotoxicity and diabetes: potential mechanisms and functional consequences. Biochem Pharmacol 2012;84:591–597
35. Smith AR, Visioli F, Frei B, Hagen TM. Age-related changes in endothelial nitric oxide synthase phosphorylation and nitric oxide dependent vasodilation: evidence for a novel mechanism involving sphingomyelinase and ceramide-activated phosphatase 2A. Aging Cell 2006;5:391–400
36. Li M, Damuni Z. I1PP2A and I2PP2A. Two potent protein phosphatase 2A-specific inhibitor proteins. Methods Mol Biol 1998;93:59–66
37. Li M, Makkinje A, Damuni Z. The myeloid leukemia-associated protein SET is a potent inhibitor of protein phosphatase 2A. J Biol Chem 1996;271:11059–11062
38. Götz J, Schild A. Transgenic and knockout models of PP2A. Methods Enzymol 2003;366:390–403
39. Bonness K, Aragon IV, Rutland B, Ofori-Acquah S, Dean NM, Honkanen RE. Cantharidin-induced mitotic arrest is associated with the formation of aberrant mitotic spindles and lagging chromosomes resulting, in part, from the suppression of PP2Aalpha. Mol Cancer Ther 2006;5:2727–2736
40. Du Y, Kowluru A, Kern TS. PP2A contributes to endothelial death in high glucose: inhibition by benfotiamine. Am J Physiol Regul Integr Comp Physiol 2010;299:R1610–R1617